AIAA JOURNAL
Vol. 37, No. 2, February 1999

Response of Composite Shells with Cutouts to Internal Pressure and Compression Loads

Mark W. Hilburger*
National Research Council, Washington, D.C. 20418
Anthony M. Waas†
University of Michigan, Ann Arbor, Michigan 48109-2118
and
James H. Starnes Jr.‡
NASA Langley Research Center, Hampton, Virginia 23681-0001

Results from a numerical study of the response of composite shells with cutouts and subjected to internal pressure and axial compression are presented. The numerical results are obtained using a geometrically nonlinear finite element code. Results for axial compression and combined internal pressure and axial compression are presented. The effects of varying internal pressure and cutout size on the prebuckling, buckling, and postbuckling responses of the shell are described. Results indicate that the nonlinear interaction between destabilizing in-plane compressive resultant stresses and out-of-plane displacements near the cutout can cause a local buckling response to occur near the cutout. The local load distributions and displacements near the cutout can be affected by the size of the cutout and by the internal pressure load. Numerical results indicate that the buckling load decreases as the size of the cutout is increased. In addition, the results indicate that the buckling load increases as the internal pressure is increased.

Introduction

MANY modern aerospace shell structures are designed to support combinations of internal pressure and mechanical loads during their service life. With the increasing need to produce lighter-weight aerospace structures, the use of advanced composite materials has become more common in the design of these structures. During operation, flight loads and internal cabin pressure are present in all commercial transport aircraft. Some of these loads may be compressive loads, and thus it is necessary to investigate the buckling characteristics of these structures. In addition, designers often need to incorporate cutouts or openings in a structure to serve as doors, windows, or access ports. It has been shown by several authors that a cutout in a shell structure subjected to axial compression can cause a significant reduction in the buckling load of the shell, e.g., Refs. 1–4. The local response near the cutout in a compression-loaded shell is strongly influenced by the local displacement gradients near the cutout and the internal load distribution. These local displacements and the internal load distribution can be affected by the size of the cutout. In addition, recent studies of the response of cylindrical shells with longitudinal cracks and subjected to internal pressure and axial compression loads, e.g., Ref. 5, indicate that the interaction between the internal pressure load and the axial compression load can have a significant effect on the local response of the structure.

The results of a numerical study of the response of quasi-isotropic cylindrical shells with a cutout and subjected to internal pressure and axial compression are presented. First, a set of dimensionless parameters governing the buckling of composite shells with cutouts is derived from the classical equations for the buckling of anisotropic thin elastic shells. The dimensionless parameters are used to characterize the results of a parametric study that is presented in this paper. These parameters help provide insight into the effects of changing geometric and laminate parameters on the buckling response of shells. The results of a parametric study using the structural analysis of general shells (STAGS) finite element code[6] are presented for three cutout sizes and five internal pressure levels to indicate the effects of cutout size and internal pressure loads on the compression response of quasi-isotropic cylindrical shells with a cutout. The predicted results are characterized by load-shortening response curves and contour plots of shell displacements and stress resultants. Finally, design curves based on classical parameters for the buckling of shells with cutouts and subjected to internal pressure and axial compression are presented.

Received Feb. 19, 1998; presented as Paper 98-1768 at the AIAA/ASME/ASCE/AHS/ASC 39th Structures, Structural Dynamics, and Materials Conference and AIAA/ASME/AHS Adaptive Structures Forum, Long Beach, CA, April 20–23, 1998; revision received Sept. 21, 1998; accepted for publication Sept. 27, 1998.

*Postdoctoral Fellow. Member AIAA.
†Associate Professor, Composite Structures Laboratory, Department of Aerospace Engineering. Associate Fellow AIAA.
‡Head, Structural Mechanics Branch. Fellow AIAA.

Classical Buckling Parameters

Nondimensional parameters governing the buckling of shells with cutouts were derived by Hilburger[4] and are summarized herein. The governing equations for the buckling of anisotropic thin elastic shells were derived from the Donnell–Mustari–Vlasov nonlinear equations in terms of curvilinear coordinates using the method of adjacent equilibrium. A nondimensionalization procedure was applied to the governing equations, producing a set of nondimensional parameters in terms of shell and cutout geometric parameters and laminate stiffnesses. The nondimensionalization procedure introduced the geometric parameters of the cutout into the equations with the following set of nondimensional coordinates:

$$X = x/a, \qquad \Theta = R\theta/b \tag{1}$$

In the case of a circular cylindrical shell, x and θ represent the axial and circumferential coordinates, respectively, and a and b are the characteristic axial and circumferential dimensions of the cutout, respectively (see Fig. 1). After some algebraic manipulation, the nondimensional transverse equilibrium equation and the compatibility equation take the following forms, respectively:

$$\alpha_b^2 \frac{\partial^4 W}{\partial X^4} + 4\alpha_b\gamma_b \frac{\partial^4 W}{\partial X^3 \partial \Theta} + 2\beta \frac{\partial^4 W}{\partial X^2 \partial \Theta^2} + 2\frac{\delta_b}{\alpha_b} \frac{\partial^4 W}{\partial X \partial \Theta^3} + \frac{1}{\alpha_b^2} \frac{\partial^4 W}{\partial \Theta^4} + \sqrt{12} C \frac{\partial^2 \Phi}{\partial X^2} - K_x \pi^2 \frac{\partial^2 W}{\partial X^2} - K_\theta \pi^2 \frac{\partial^2 W}{\partial \Theta^2} - \frac{K_{x\theta}\pi^2}{\alpha_b} \frac{\partial^4 W}{\partial X \partial \Theta} = 0 \tag{2}$$

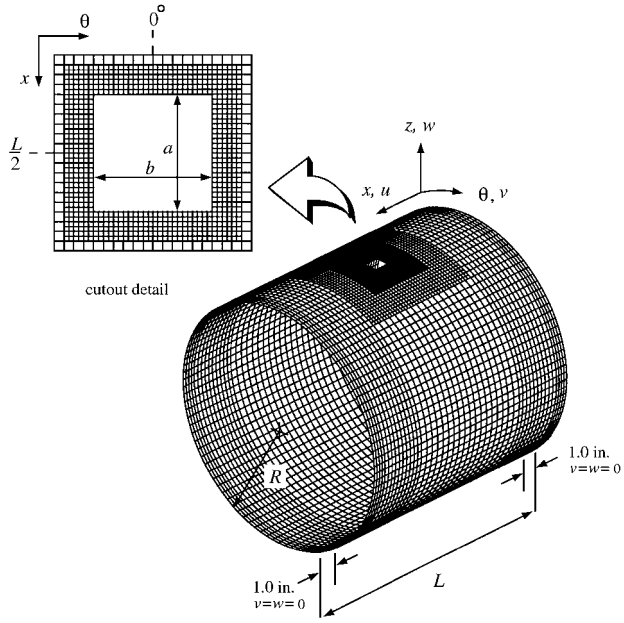

Fig. 1 Typical shell model.

and

$$\alpha_m^2 \frac{\partial^4 \Phi}{\partial X^4} + 2\alpha_m \gamma_m \frac{\partial^4 \Phi}{\partial X^3 \partial \Theta} + 2\mu \frac{\partial^4 \Phi}{\partial X^2 \partial \Theta^2} + 2\frac{\delta_m}{\alpha_m} \frac{\partial^4 \Phi}{\partial X \partial \Theta^3} + \frac{1}{\alpha_m^2} \frac{\partial^4 \Phi}{\partial \Theta^4} = \sqrt{12} C \frac{\partial^2 W}{\partial X^2} \tag{3}$$

where Φ is a stress resultant function and W is a nondimensional buckling displacement. The remaining parameters in Eq. (2) are nondimensional bending parameters and buckling coefficients defined by

$$\alpha_b = \frac{b}{a}\left(\frac{D_{11}}{D_{22}}\right)^{\frac{1}{4}} \tag{4}$$

$$\beta = \frac{D_{12} + 2D_{66}}{\sqrt{D_{11} D_{22}}} \tag{5}$$

$$\gamma_b = \frac{D_{16}}{\left(D_{11}^3 D_{22}\right)^{\frac{1}{4}}} \tag{6}$$

$$\delta_b = \frac{D_{26}}{\left(D_{11} D_{22}^3\right)^{\frac{1}{4}}} \tag{7}$$

$$K_x = \frac{N_x^0 b^2}{\pi^2 \sqrt{D_{11} D_{22}}} \tag{8}$$

$$K_\theta = \frac{N_\theta^0 a^2}{\pi^2 \sqrt{D_{11} D_{22}}} \tag{9}$$

$$K_{x\theta} = \frac{N_{x\theta}^0 b^2}{\pi^2 \left(D_{11} D_{22}^3\right)^{\frac{1}{4}}} \tag{10}$$

where D_{11}, D_{12}, D_{22}, D_{16}, D_{26}, and D_{66} are the shell bending stiffnesses found in classical laminated shell theory. The terms N_x^0, N_θ^0, and $N_{x\theta}^0$ are the prebuckling in-plane stress resultants. The remaining parameters in Eq. (3) are nondimensional membrane parameters and a cutout or curvature parameter C in terms of shell membrane stiffnesses A_{11}, A_{12}, A_{22}, D_{16}, D_{26}, and A_{66}. In the special case of balanced symmetric laminates with A_{16} and A_{26} equal to zero, these parameters are

$$\alpha_m = \frac{b}{a}\left(\frac{A_{11}}{A_{22}}\right)^{\frac{1}{4}} \tag{11}$$

Table 1 Lamina material properties

E_1, Mpsi	E_2, Mpsi	G_{12}, Mpsi	ν_{12}
21.5	1.61	0.93	0.295

$$\mu = \frac{A_{11}A_{22} - A_{12}^2 - 2A_{12}A_{66}}{2A_{66}\sqrt{A_{11}A_{22}}} \tag{12}$$

$$C = \frac{b^2}{R}\left[\frac{A_{11}A_{22} - A_{12}^2}{12\sqrt{A_{11}A_{22}D_{11}D_{22}}}\right]^{\frac{1}{4}} \tag{13}$$

and $\gamma_m = 0$ and $\delta_m = 0$.

In the context of this paper, in which shells are subjected to internal pressure loading P_{int}, it is useful to introduce the relation $N_\theta^0 = P_{\text{int}} R$. This relation is derived from the membrane solution for a circular cylindrical shell subjected to internal pressure.

Cylinder Models and Analysis Methods

Cylinder Model

The STAGS finite element analysis code[6] was used to predict the response of the shells. A typical finite element model of the shells analyzed in this study is described in Fig. 1. A typical model contains approximately 7800 nodes with six degrees of freedom per node and 6820 quadrilateral shell elements. The shells have a radius of 8.0 in. and are 16.0 in. long. The shells have an eight-ply $[\pm 45/0/90]_s$ quasi-isotropic wall lamination. The ply thickness is assumed to be 0.005 in., resulting in a total laminate thickness of 0.04 in. The lamina properties are summarized in Table 1. A square cutout is located at $\theta = 0$ deg, at the shells' midlength. The cutouts considered in this study include 0.5×0.5, 1.0×1.0, and 1.5×1.5 in. square cutouts. The axial and circumferential dimensions of the cutout are denoted by a and b, respectively, as indicated in Fig. 1. An idealized version of typical experimental boundary conditions was included in the model by constraining circumferential and radial degrees of freedom v and w, respectively, in regions of the shell between 0.0 in. $\geq x \geq$ 1.0 in. and 15.0 in. $\geq x \geq$ 16.0 in., as illustrated in Fig. 1. The resulting shell has a total unsupported length of 14.0 in.

The loading conditions studied include axial compression and combined axial compression and internal pressure. For the axial compression cases, a compression load was applied to the shell by a uniform axial displacement. For the combined internal pressure and axial compression cases, a live pressure load was applied to the shell first, and then an axial compression load was applied to the pressurized shell. Pressure levels equal to 5.0, 10.0, 20.0, 30.0, and 50.0 psi were applied to the shell for the combined load cases. The internal pressure was simulated by applying a uniform lateral pressure to the shell wall and an axial tension load to the end of the shell. Multipoint constraints were applied to the ends of the shell to enforce uniform displacement.

Nonlinear Analysis Methods

The quasistatic compression response of the shells was determined using a standard arclength projection method[7] in STAGS. The arclength method is often sufficient for predicting results beyond instability points in the response. However, for cases where the standard arclength method failed to converge to solutions beyond instability points, a nonlinear transient analysis method[8] was used in the analysis. The transient analysis in STAGS includes a numerical time integration scheme developed by Park[9] and proportional structural damping. The material density used in the finite element calculations is 0.057 lb/in.^{3}. The transient analysis was initiated at an unstable equilibrium point just beyond the instability point by applying an increment to the end-shortening displacement. The transient analysis was continued until the kinetic energy in the system was dissipated to a negligible level by the structural damping. A load relaxation procedure was then applied to the system to establish a stable equilibrium state from which a quasistatic analysis could be resumed. A typical finite element analysis required 11 to 17 h on an engineering CPU workstation.

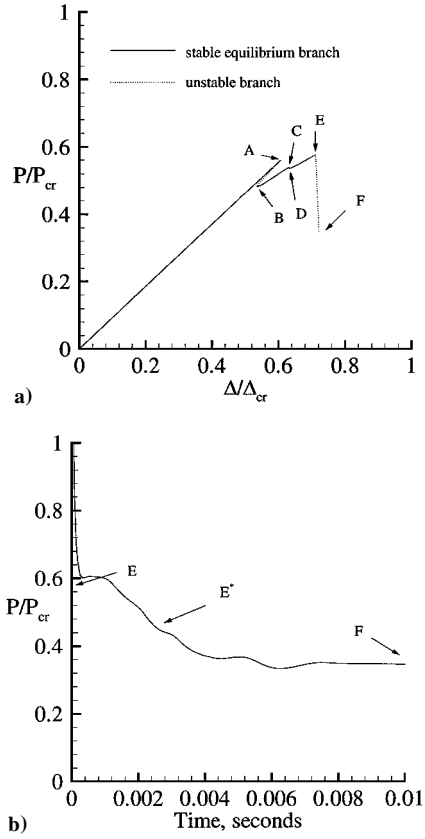

Fig. 2 Compression response of a quasi-isotropic shell with a 1.0 × 1.0 in. square cutout: a) load-shortening response and b) load time history of the unstable collapse response associated with segment E-F in Fig. 2a.

Results and Discussion

Results from a numerical study of the response of quasi-isotropic laminated shells with a cutout are presented in this section. Two loading conditions were considered in this study and include axial compression only and a combination of internal pressure and axial compression loads. Results have been generated for cutouts at the shell midlength including 0.5 × 0.5, 1.0 × 1.0, and 1.5 × 1.5 in. square cutouts. Results have been generated for internal pressure loads of 5.0, 10.0, 20.0, 30.0, and 50.0 psi. First, results from a representative shell are presented to identify typical response characteristics of a shell with a cutout and subjected to axial compression. Results illustrating the effects of internal pressure on the compression response are presented. Finally, design curves are presented summarizing the effects of internal pressure on the initial buckling loads of shells with square cutouts.

Axial Compression Loads

Results for a quasi-isotropic $[\pm 45/0/90]_s$ shell with a 1.0 × 1.0 in. square cutout are presented to identify typical response characteristics of a compression-loaded shell with a square cutout. A load-shortening response curve is given in Fig. 2a as an overall guide to the compression response. An extensive postbuckling response is indicated by a number of stable and unstable segments in the load-shortening results. The initial buckling point is labeled A, and the additional extreme points are labeled B, C, D, etc. The postbuckling response includes both stable segments (e.g., B–C and D–E) and unstable segments (e.g., A–B, C–D, and E–F), as shown in Fig. 2a. Segments A–B and C–D are associated with unstable local buckling events that occur near the cutout. These buckling events result in large out-of-plane deformations and rapidly varying stress gradients near the cutout. Stable postbuckling segments B–C and D–E are accompanied by an increase in the magnitude of the local deformations in the shell near the cutout. The overall collapse of the shell occurs at point E, and the unstable collapse response

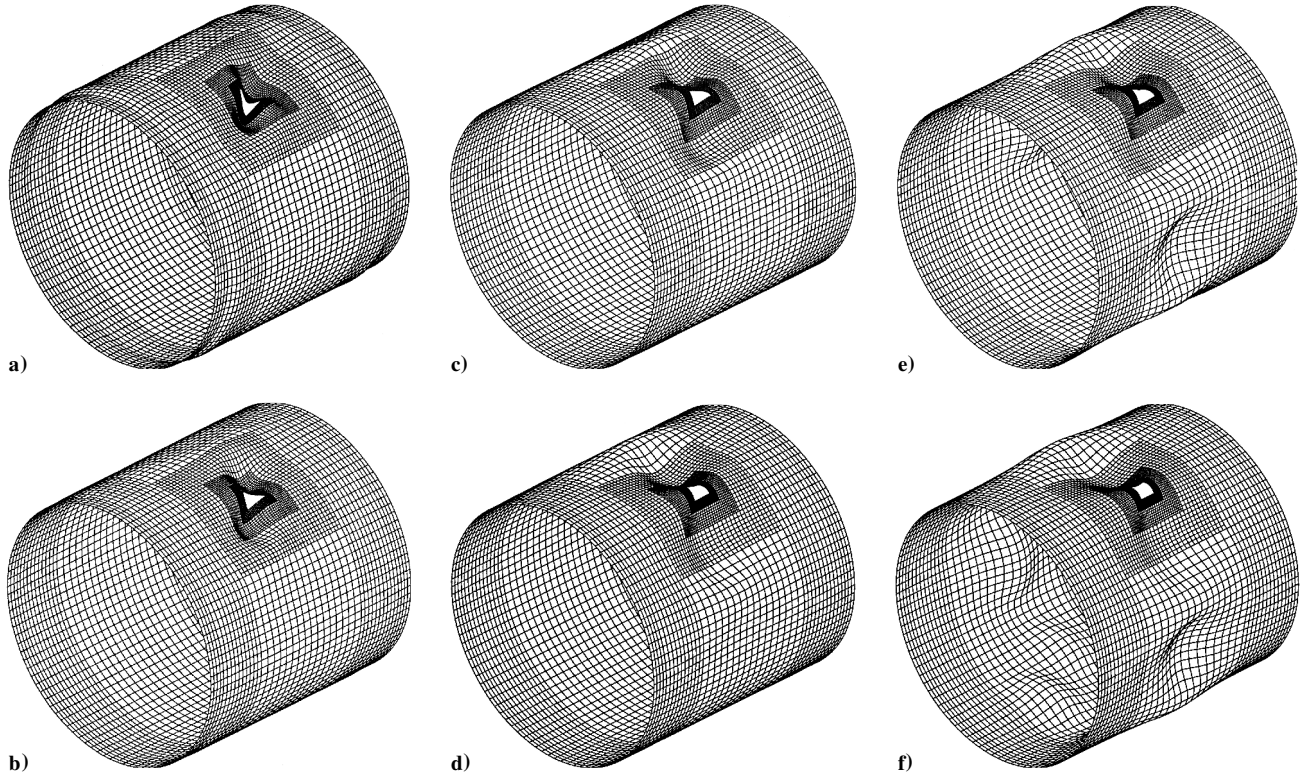

Fig. 3 Selected deformation patterns for a compression-loaded quasi-isotropic shell with a 1.0 × 1.0 in. square cutout: a) point A, b) point B, c) point C, d) point E, e) point E*, and f) point F (refer to Fig. 2 for selected points).

is represented by segment E–F. The collapse response is characterized by a significant reduction in load and the development of the general instability mode in the shell. The load time history of the collapse response is shown in Fig. 2b. Furthermore, the results indicate that the slope of each adjacent stable equilibrium segment of the response curve decreases as loading continues in the postbuckling range, indicating a reduction in the effective axial compression stiffness of the shell. This decrease in effective axial stiffness is due to the increasingly large deformations that develop in the shell throughout the compression response, which result in significant stress redistribution away from the cutout.

Deformation patterns corresponding to selected extreme points on the load-shortening response curve are shown in Figs. 3a–3f. Figure 3a shows the displacements associated with the initial buckling point A, consisting of an elliptical-shaped inward buckle at the cutout with the semimajor axis aligned in a helical or skew direction. The postbuckling deformation pattern associated with point B consists of large elliptical-shaped buckles on either side of the cutout. Deformation patterns in Figs. 3c and 3d indicate that, as the postbuckling response progresses, the elliptical buckles in the shell become increasingly well defined and the buckle pattern rotates counterclockwise around the cutout. Figure 3e shows an intermediate deformation pattern associated with point E* during the collapse response of the shell. The deformation pattern indicates that additional buckles propagate around the circumference of the shell during the response until the general instability collapse mode forms, as shown in Fig. 3f.

Contour plots of axial and circumferential stress resultants corresponding to buckling point A in Fig. 2a are shown in Figs. 4a and 4b, respectively. The results indicate that rapidly varying stress gradients form near the cutout and quickly decay to far-field values away from the cutout. In addition, the results indicate that regions of destabilizing in-plane biaxial compression form near the cutout. These regions of destabilizing stresses couple with the out-of-plane deformations near the cutout to cause the local buckling response. In-plane stress resultants associated with the global collapse configuration are shown in Figs. 5a and 5b. The stress contours indicate that significant stress redistribution occurs in the shell as a result of the large out-of-plane deformations that develop.

The results indicate that variations in the size of the cutout can have a significant effect on the compression response of a shell with a cutout. The load-shortening relations for shells with 0.5×0.5,

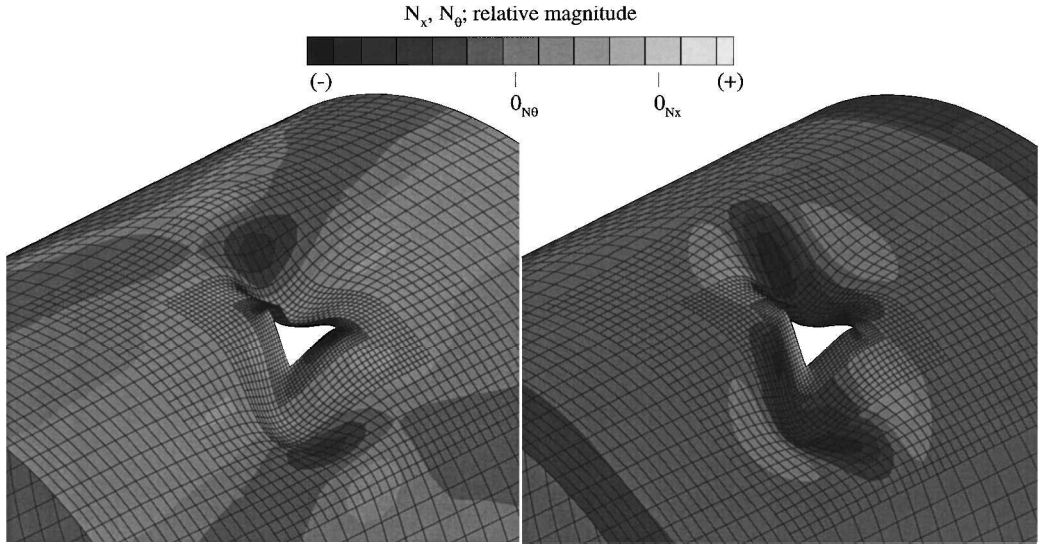

a) N_x b) N_θ

Fig. 4 Buckling stress resultants for a compression-loaded shell with a 1.0 × 1.0 in. square cutout: a) axial stress resultant and b) circumferential (hoop) stress resultant (magnified view).

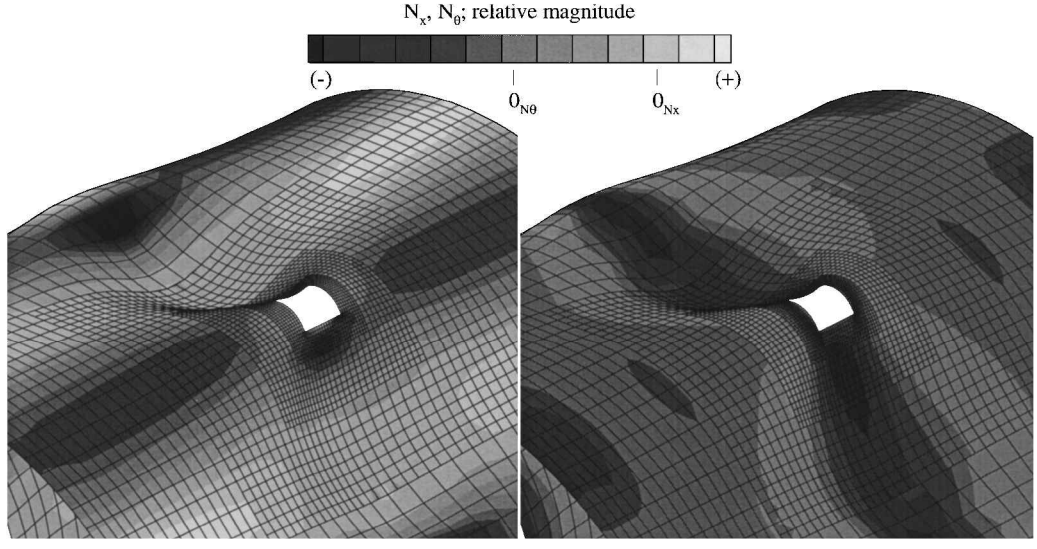

a) N_x b) N_θ

Fig. 5 General instability stress resultants for a compression-loaded shell with a 1.0 × 1.0 in. square cutout: a) axial stress resultant and b) circumferential (hoop) stress resultant (magnified view).

1.0 × 1.0, and 1.5 × 1.5 in. square cutouts are shown in Fig. 6. The results indicate that the magnitude of the initial buckling load decreases as the cutout size increases. The values of the normalized buckling loads are 0.83, 0.56, and 0.45 for the 0.5 × 0.5, 1.0 × 1.0, and 1.5 × 1.5 in. square cutouts, respectively. This decrease in the magnitude of the buckling load as the cutout size increases is due to the formation of larger prebuckling out-of-plane displacements and in-plane destabilizing compressive stresses near the cutout at lower applied loads, causing a local buckling response near the cutout at lower applied load levels. For shells with 1.0 × 1.0 and 1.5 × 1.5 in. cutouts, the initial buckling response results in a stable local postbuckling state, and additional load can be applied to the shell before the overall collapse occurs. For the 0.5 × 0.5 in. square cutout, the initial local buckling event appears to be enough of a lateral disturbance to the shell to cause the overall collapse of the shell immediately following the local buckling event.

Internal Pressure and Axial Compression Loads

The effects of internal pressure on the compression response of a shell with a 1.0 × 1.0 in. square cutout are summarized in Figs. 7a and 7b. The results indicate that the magnitude of the first local buckling loads of the shells increase with an increase in the internal pressure. The values of the normalized local buckling loads for the shell with the 1.0 × 1.0 in. cutout and internal pressure levels of 0.0, 10.0, 30.0, and 50.0 psi are 0.56, 0.64, 0.70, and 0.79, respectively. The internal pressure retards the formation of the regions of destabilizing biaxial compression near the cutout that were described in the discussion of the axial-compression-only case and, hence, retards the onset of the local buckling of the shell. In addition, the results indicate that an increase in the internal pressure causes a decrease in the magnitude of the postbuckling load reduction. This trend continues until a value of internal pressure is reached for which the first local buckling response no longer exhibits an unstable local buckling response. For these results, shells with an internal pressure greater than or equal to 30 psi have a stable first local buckling response accompanied by a gradual development of large out-of-plane deformations and rapidly varying stress gradients near the cutout. Furthermore, the results show that the general instability load for the shells increases and the magnitude of the collapse load reduction decreases as the level of internal pressure increases.

A typical example of the initial postbuckling deformation pattern for a shell with a 1.0 × 1.0 in. cutout and subjected to 30 psi of internal pressure and axial compression is shown in Fig. 8a. The results indicate that the internal pressure significantly influences the character of the local shell deformations near the cutout when compared with the results for axial compression only. The displacements are characterized by large out-of-plane local bending of the

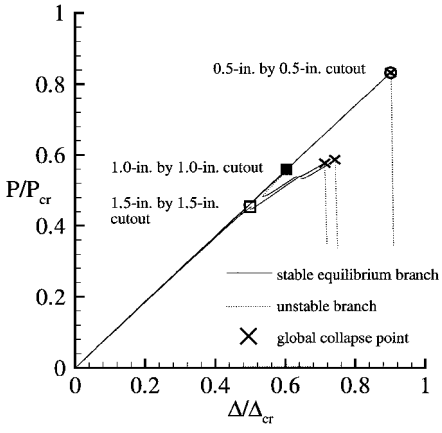

Fig. 6 Effect of cutout size on the response of a quasi-isotropic shell subjected to axial compression.

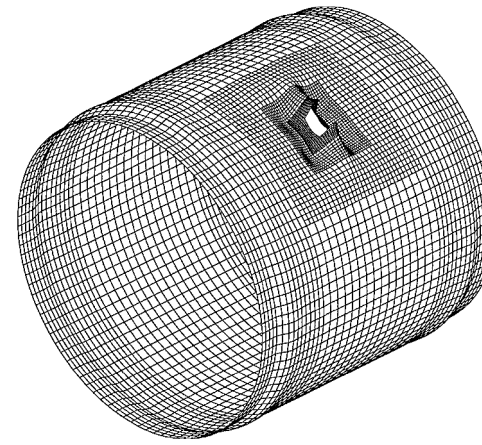

a) Initial postbuckling pattern

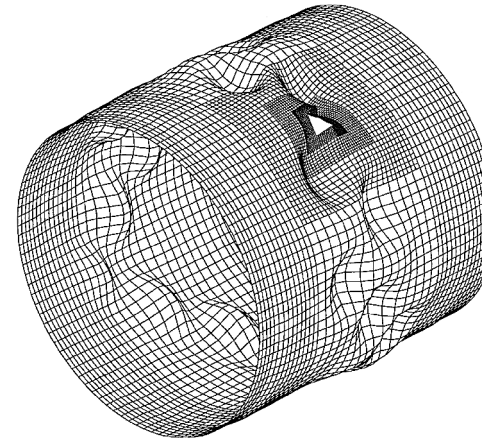

b) General instability deformation pattern

Fig. 8 Selected deformation patterns for a quasi-isotropic shell with a 1.0 × 1.0 in. square cutout and subjected to 30 psi of internal pressure and axial compression.

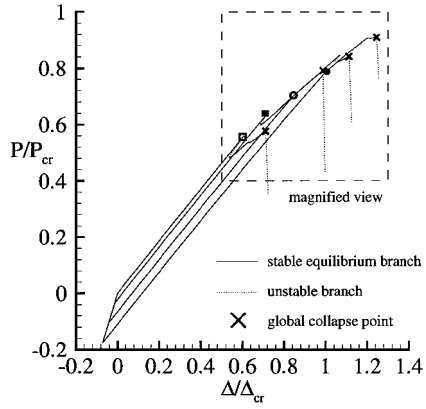

a) Load-shortening response

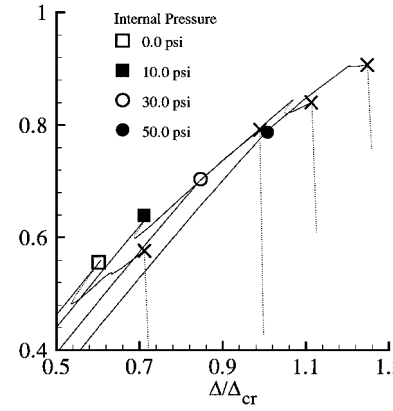

b) Magnified view of local and global buckling events

Fig. 7 Effects of internal pressure on the response of a quasi-isotropic shell with a 1.0 × 1.0 in. square cutout.

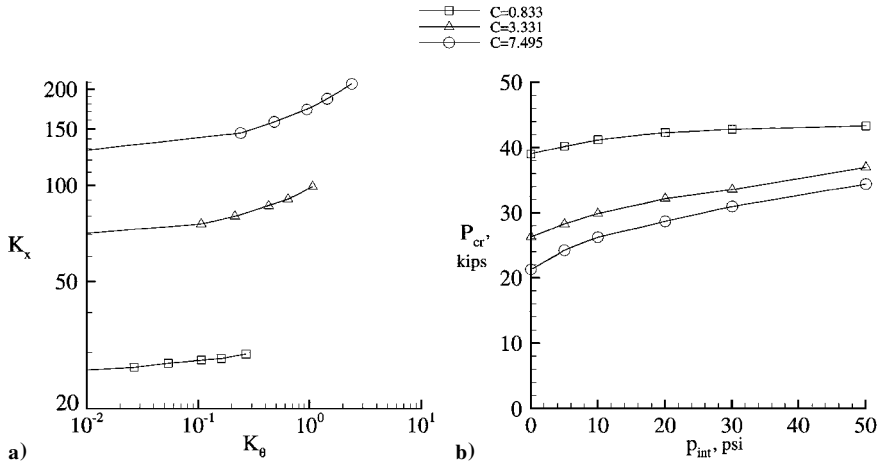

Fig. 9 Design curves for the initial buckling load of a shell with a cutout and subjected to internal pressure and axial compression.

axially aligned edges of the cutout. The general instability collapse mode for the same shell is shown in Fig. 8b, which indicates that an increase in the internal pressure causes an increase in the number of axial and circumferential half-waves of the collapse mode shape.

Design curves for the initial buckling load of shells with square cutouts and subjected to internal pressure are presented in Figs 9a and 9b. The relation between the axial and circumferential nondimensional loading factors K_x and K_θ, respectively, for three values of the cutout or curvature parameter C and $\alpha_b = 1.064$, $\beta = 1.936$, $\gamma_b = 0.176$, and $\delta_b = 0.200$ are shown in Fig. 9a. Additional information about the initial buckling loads of these shells is obtained from Fig. 9b. The results indicate that the initial buckling load of a shell with a cutout increases as the internal pressure increases, as discussed previously. Furthermore, the results indicate that the increase in internal pressure in a shell with a cutout will result in a larger increase in the initial buckling load for larger values of the parameter C. The curves indicate that the nondimensional parameters can be useful in summarizing the results in terms of nondimensional design curves. The nondimensional parameters and design curves can provide a convenient format in which a designer can determine the effects of individual design parameters on the buckling response of the shell.

Concluding Remarks

The results of a numerical study of the response of quasi-isotropic laminated shells with square cutouts subjected to axial compression and combined internal pressure and axial compression loads are presented. The results indicate that a nonlinear interaction between destabilizing in-plane compressive stresses and out-of-plane deformations near a cutout in a compression-loaded shell causes a local buckling response to occur near the cutout. For sufficiently large cutouts, the local buckling response exhibits an unstable buckling event followed by a stable postbuckling state consisting of large out-of-plane deformations and rapidly varying in-plane stress gradients. For sufficiently small cutouts, the local buckling response produces enough of a lateral disturbance to the shell to cause the overall collapse of the shell. The results indicate that an increase in the size of the cutout can cause a significant reduction in the initial buckling load of the shell and a reduction in the magnitude of the postbuckling load reduction. The reduction in the buckling load with an increase in the cutout size is due to the formation of larger prebuckling deformations and in-plane destabilizing stresses near the cutout at lower applied loads, which, in turn, causes a local buckling response to occur near the cutout at lower-applied-load levels. The results indicate that the response of a compression-loaded cylinder is strongly influenced by an internal pressure load. An increase in the internal pressure causes an increase in the initial buckling load of the shell and the general instability load of the shell. Increasing the internal pressure retards the formation of destabilizing in-plane compressive stresses near the cutout and, hence, retards the onset of the local buckling response. Numerically generated design curves and nondimensional parameters are presented, offering a convenient format for summarizing the initial buckling loads of shells with cutouts and subjected to internal pressure and axial compression. The design curves and the dimensionless parameters should be useful for the future design of aerospace shell structures with cutouts by enabling a designer to compare the effects of variations in material properties and structural geometric variables on the buckling response of the shell.

Acknowledgments

This work was supported by the NASA Graduate Student Researchers Program and NASA Langley Research Center Grant NGT-57256.

References

[1] Brogan, F., and Almroth, B. O., "Buckling of Cylinders with Cutouts," *AIAA Journal*, Vol. 8, No. 2, 1970, pp. 236–240.

[2] Tennyson, R. C., "The Effects of Unreinforced Circular Cutouts on the Buckling of Circular Cylindrical Shells," *Journal of Engineering for Industry*, Vol. 90, Nov. 1968, pp. 541–546.

[3] Starnes, J. H., "The Effect of a Circular Hole on the Buckling of Cylindrical Shells," Ph.D. Dissertation, Dept. of Aeronautics, California Inst. of Technology, Pasadena, CA, June 1970.

[4] Hilburger, M. W., "Numerical and Experimental Study of the Compression Response of Composite Cylindrical Shells with Cutouts," Ph.D. Dissertation, Dept. of Aerospace Engineering, Univ. of Michigan, Ann Arbor, MI, April 1998.

[5] Starnes, J. H., and Rose, C. A., "Nonlinear Response of Thin Cylindrical Shells with Longitudinal Cracks and Subjected to Internal Pressure and Axial Compression Loads," AIAA Paper 97-1144, April 1997.

[6] Brogan, F. A., Rankin, C. C., and Cabiness, H. D., "STAGS User Manual," Lockheed Palo Alto Research Lab., Advanced Technology Center, Rept. LMSC P032594, Palo Alto, CA, June 1998.

[7] Riks, E., "The Application of Newton's Method to the Problem of Elastic Stability," *Journal of Applied Mechanics*, Vol. 39, Dec. 1972, pp. 1060–1066.

[8] Riks, E., Rankin, C. C., and Brogan, F. A., "On the Solution of Mode Jumping Phenomena in Thin-Walled Shell Structures," *Computational Methods in Applied Mechanics and Engineering*, Sept. 1996, pp. 59–92.

[9] Park, K. C., "An Improved Stiffly Stable Method for Direct Integration of Nonlinear Structural Dynamics," *Journal of Applied Mechanics*, Vol. 42, June 1975, pp. 464–470.

G. M. Faeth
Editor-in-Chief